

# Atmospheric convection with condensation of the major component

Tatsuya Yamashita<sup>\*</sup>, Masatsugu Odaka<sup>\*</sup>, Ko-ichiro Sugiyama<sup>\*\*,†</sup>, Kensuke Nakajima<sup>\*\*\*</sup>,  
Masaki Ishiwatari<sup>\*,‡</sup>, Yoshi-Yuki Hayashi<sup>†,‡</sup>

<sup>\*</sup> Department of CosmoSciences, Graduate School of Science, Hokkaido University

<sup>\*\*</sup> Institute of Low Temperature Science, Hokkaido University

<sup>\*\*\*</sup> Department of Earth and Planetary Sciences, Faculty of Sciences, Kyushu University

<sup>†</sup> Department of Earth and Planetary Sciences, Graduate School of Science, Kobe University

<sup>‡</sup> Center for Planetary Science

## 1 Introduction

In Martian atmosphere, atmospheric major component, CO<sub>2</sub>, condenses. In current Martian polar regions, CO<sub>2</sub> ice clouds are known to exist, and there is a possibility that these clouds are formed by convective motion (Colaprete *et al.*, 2003). Pollack *et al.* (1987) and Kasting(1991) proposed that the early Martian atmosphere was thicker than present one, and that large amounts of CO<sub>2</sub> ice cloud existed. Studies on the early Martian climate suggested that the scattering greenhouse effect of CO<sub>2</sub> ice clouds had a highly significant effect on the climate (Forget and Pierrehumbert, 1997; Mitsuda, 2007).

In a system whose major component condenses, the degrees of freedom for thermodynamic variables degenerate when supersaturation does not occur. Due to degeneracy of degree of freedom, temperature profile of ascent region must be equal to that of descent region, and air parcel can not obtain buoyancy. Thus, it is thought that moist convection does not develop. On the other hand, if supersaturation occurs, temperature profile of ascent region is not necessarily equal to that of descent region. In that case, there is a possibility that moist convection develops.

Laboratory experiments and observations from orbiters suggested existence of highly supersaturated regions in Martian atmosphere (Glandorf *et al.*, 2002; Colaprete *et al.*, 2003). Colaprete *et al.* (2003) considered that moist convection does not develop when supersaturation does not occur, and performed calculations under the condition that supersaturation occurs. They showed that moist convection develops when supersaturation occurs. However, the model used by Co-

laprete *et al.* (2003) was vertical one dimensional, and there was an uncertainty in the parameterizations related to the effects of entrainment and pressure gradient. In order to investigate the structure of the convection which is established through a large number of life cycles of convective cloud elements, cloud convection model which explicitly consider the convective motion should be used.

We have been developing a cloud convection model in order to investigate atmospheric convective structure in various planets (e.g., Nakajima *et al.*, 2000; Odaka *et al.*, 2006; Sugiyama *et al.*, 2009). Odaka *et al.* (2006) incorporated the effects of condensation of major component into the cloud convection model, and performed numerical experiments of ascending hot plume as a test calculation under Martian atmospheric condition. Yamashita *et al.* (2009) incorporated a simple radiation scheme which ensures the balance between heating and cooling, and a condensation scheme which allows for supersaturation to occur. They performed long time integration in order to investigate cloud structure in statistical equilibrium states under the same initial temperature profile as Odaka *et al.* (2006). They suggested that the presence or absence of supersaturation causes significant difference of structure of moist convection. However, recently we found that there are several bugs in the radiation scheme and the condensation scheme which Yamashita *et al.* (2009) incorporated. These bugs cause atmospheric temperature increase at any level and nonconservation of total mass of gas and cloud. In this paper, we report the result of recalculation of Yamashita *et al.* (2009) by using the modified programs.

## 2 Model description

We assume that atmosphere consists entirely of CO<sub>2</sub>. The governing equations are the quasi-compressible equations by Klemp and Wilhelmson(1978) with additional terms representing major component condensation (Odaka *et al.*, 2005). The model used here is two-dimensional in the horizontal and vertical directions. The equations of motion, the pressure equation, the thermodynamic equation, and the conservation law for cloud are written as

$$\frac{du'}{dt} = -c_p \bar{\theta} \frac{\partial \pi'}{\partial x} + D_m(u'), \quad (1)$$

$$\frac{dw'}{dt} = -c_p \bar{\theta} \frac{\partial \pi'}{\partial z} + g \frac{\theta'}{\bar{\theta}} + D_m(w'), \quad (2)$$

$$\begin{aligned} \frac{\partial \pi'}{\partial t} + \frac{R\bar{\pi}}{c_v \bar{\rho} \bar{\theta}} \left[ \frac{\partial(\bar{\rho} \bar{\theta} u')}{\partial x} + \frac{\partial(\bar{\rho} \bar{\theta} w')}{\partial z} \right] \\ = \frac{R\bar{\pi}}{c_v \bar{\rho}} \left( \frac{L}{c_p \bar{\theta} \bar{\pi}} - 1 \right) M_c \\ + \frac{R}{c_v \bar{\theta}} (Q_{dis} + Q_{rad}), \end{aligned} \quad (3)$$

$$\begin{aligned} \frac{d\theta'}{dt} + w' \frac{\partial \bar{\theta}}{\partial z} = \frac{1}{\bar{\pi}} \left( \frac{LM_c}{\bar{\rho} c_p} + Q_{dis} + Q_{rad} \right) \\ + D_h(\theta'), \end{aligned} \quad (4)$$

$$\begin{aligned} \frac{\partial \rho'_s}{\partial t} + \frac{\partial(\rho'_s u')}{\partial x} + \frac{\partial(\rho'_s w')}{\partial z} \\ = M_c + D_h(\rho_s), \end{aligned} \quad (5)$$

where

$$\frac{d}{dt} = \frac{\partial}{\partial t} + u' \frac{\partial}{\partial x} + w' \frac{\partial}{\partial z}, \quad (6)$$

$$D_m(\cdot) = \frac{\partial}{\partial x} \left[ K_m \frac{\partial(\cdot)}{\partial x} \right] + \frac{1}{\bar{\rho}} \frac{\partial}{\partial z} \left[ \bar{\rho} K_m \frac{\partial(\cdot)}{\partial z} \right], \quad (7)$$

$$D_h(\cdot) = \frac{\partial}{\partial x} \left[ K_h \frac{\partial(\cdot)}{\partial x} \right] + \frac{1}{\bar{\rho}} \frac{\partial}{\partial z} \left[ \bar{\rho} K_h \frac{\partial(\cdot)}{\partial z} \right]. \quad (8)$$

$u$  and  $w$  are horizontal and vertical component of velocity, respectively.  $\rho$  is gas density,  $\rho_s$  is cloud density, and  $T$  is temperature.  $\pi$  is the Exner function,

$$\pi = \left( \frac{p}{p_0} \right)^{R/c_p}. \quad (9)$$

$\theta$  is potential temperature,

$$\theta = \frac{T}{\pi}. \quad (10)$$

Overbar denotes the basic state which depends only on height, and prime denotes the perturbation components.  $K_m$  and  $K_h$  are eddy coefficients for momentum and scalar variables, respectively.  $Q_{dis}$  is heating rate of dissipation.  $K_m$ ,  $K_h$  and  $Q_{dis}$  are calculated by using 1.5 order closure (Klemp and Wilhelmson, 1978).

$Q_{rad}$  is radiative heating rate,  $M_c$  is condensation rate, and  $L$  is latent heat of fusion.  $c_p$  and  $c_v$  are the specific heat at constant pressure and volume, respectively.  $R$  is the gas constant for unit mass,  $g$  is gravitational acceleration, and  $p_0$  is surface pressure.

We do not calculate radiation transfer explicitly, but we give horizontally uniform heating and cooling  $Q_{rad}$ . Cooling rate is fixed at constant value  $q_{cool}$ , and heating rate  $q_{heat}(t)$  is adjusted to retain  $\int_{z_b}^{z_t} \rho Q_{rad} dz = 0$ , where  $z_b$ ,  $z_t$  are lower and upper level of computational domain. Then  $Q_{rad}$  is given by

$$Q_{rad}(z, t) = \begin{cases} q_{heat}(t), & (z_1 \leq z \leq z_2) \\ q_{cool}, & (z_3 \leq z \leq z_4) \\ 0, & (\text{otherwise}) \end{cases} \quad (11)$$

where  $z_1$ ,  $z_2$  are lower and upper levels of cooling layer, and  $z_3$ ,  $z_4$  are lower and upper levels of heating layer.  $q_{heat}(t)$  is given by

$$q_{heat}(t) = -q_{cool} \times \frac{\int_{z_3}^{z_4} \rho dz}{\int_{z_1}^{z_2} \rho dz}. \quad (12)$$

The radiation scheme of Yamashita *et al.*(2009) did not satisfy (12), and this bug is fixed in this study. Neither surface fluxes of momentum nor heat are considered in our model.

Condensation of CO<sub>2</sub> occurs when saturation ratio  $S = p/p_*$  exceeds critical saturation ratio  $S_{cr}$ , the ratio of pressure  $p$  to saturation vapor pressure  $p_*$  in onset of condensation.  $p_*$  is given by

$$p_* = \exp \left( A_{ant} - \frac{B_{ant}}{T - C_{ant}} \right), \quad (13)$$

where  $A_{ant} = 27.4$ ,  $B_{ant} = 3103$  K,  $C_{ant} = -0.16$  K (The society of chemical engineers of Japan, 1999). Since  $T \gg |C_{ant}|$ , we assume that  $C_{ant} \sim 0$  as Tobie *et al.* (2003) did. We assume that cloud particles grow by diffusion process, and the effect of growth by coalescence process is not considered. Condensation rate  $M_c$  is expressed by Tobie *et al.* (2003)'s formulation with a threshold for inhibiting unphysical condensation(Yamashita *et al.*,2009);

$$\begin{aligned} M_c &= \frac{4\pi r N k_d R T^2}{L^2} (S - 1) \\ &\text{if } \begin{cases} S > S_{cr} \\ \text{or } S \leq 1, \rho_s \neq 0 \\ \text{or } 1 < S \leq S_{cr}, \rho_s > \varepsilon, \end{cases} \end{aligned} \quad (14)$$

where  $r$  is cloud particle radius(determined by (15)),  $N$  is number density of condensation nuclei, and  $k_d$  is heat conduction coefficient. We use the value of  $k_d = 4.8 \times 10^{-3} \text{ W K}^{-1} \text{ m}^{-1}$  (Tobie *et al.*, 2003).  $\varepsilon$  is a threshold constant for inhibiting unphysical condensation which can occur when saturation ratio is large. From (13) and Clausius-Clapeyron equation, latent heat  $L$  is constant value:  $L = B_{ant}R$ .

We assume that cloud particles radii  $r$  in one grid domain are constant, and  $r$  is expressed by cloud density  $\rho'_s$  and condensation nucleus radius  $r_d$  :

$$r = \left( r_d^3 + \frac{3\rho'_s}{4\pi N\rho_I} \right)^{1/3}, \quad (15)$$

where  $\rho_I$  is the density of  $\text{CO}_2$  ice, and we take  $\rho_I = 1.565 \times 10^3 \text{ kg/m}^3$  (National Astronomical Observatory of Japan, 2004).  $r_d$  is  $0.1 \mu\text{m}$ , and number density of condensation nucleus per unit mass of air in basic state  $N/\bar{\rho}$  is  $5.0 \times 10^8 \text{ kg}^{-1}$  (Tobie *et al.*, 2003).

In this simulation, we do not consider falling of cloud particle and drag force due to cloud particles.

For space discretization, we use fourth order centered difference for advection terms, and second order centered difference for the other terms. Solving the advection term of cloud density by using centered difference causes negative cloud density. When negative cloud density occurs in a grid point, positive cloud density is transferred from surrounding points to the point so that the cloud density at the point is zero. This procedure is added in the course of improving the condensation scheme of Yamashita *et al.*(2009).

In order to save computational resources, time-splitting method is used in our calculation. The terms associated with sound wave and condensation is treated by the HE-VI scheme using a short time step. In the horizontal direction, explicit scheme(Euler scheme) is used, and in the vertical direction, implicit scheme (Crank-Nicolson scheme) is used. The other terms are treated by the leap-frog scheme with Asselin time filter(Asselin, 1972) using a long time step. The coefficient of Asselin time filter is 0.1. Artificial viscosity terms are introduced for the sake of calculation stability.

Developed numerical models and documents are available in <http://www.gfd-dennou.org/library/deepconv/>.

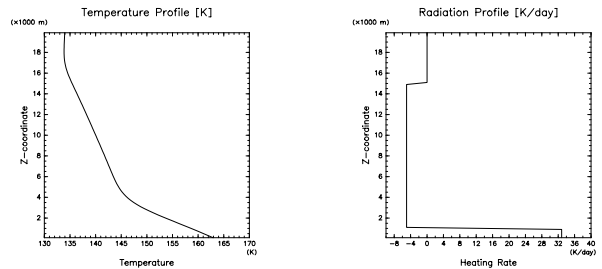


Figure 1: Initial temperature profile (left panel) and initial profile of heating rate(right panel).

### 3 Numerical configuration

The computational domain is 50 km in the horizontal direction and 20 km in the vertical direction. Grid spacing is 200 m. Short time step is 0.125 sec, and long time step is 1.0 sec. We set surface pressure and temperature to be 7 hPa and 165 K, respectively. We use periodic boundary condition in horizontal direction and stress-free boundary condition in vertical direction. We give an initial temperature profile on the basis of a temperature profile in Martian winter polar cap (Colaprete and Toon, 2002). In this profile, temperature follows the dry adiabatic lapse rate below 4 km height, and follows the saturation vapor pressure from 4 km height to 15 km height, and is nearly constant (134 K) above 15 km height (Fig.1 left). We determine the initial pressure profile based on hydrostatic equation. As initial perturbation, random noise of potential temperature with amplitude of 1 K is added to the lowest layer of atmosphere. As for the level of radiative heating and cooling, we give  $z_1 = 0 \text{ m}$ ,  $z_2 = 1000 \text{ m}$ ,  $z_3 = 1000 \text{ m}$ ,  $z_4 = 15000 \text{ m}$  in (12). Cooling rate is set to be  $q_{cool} = -5.0 \text{ K/day}$  (Fig.1 right).

Critical saturation ratio  $S_{cr}$  in our calculation is 1.0. Integration time is  $8.64 \times 10^5 \text{ sec}$  (10 days).

### 4 Results

At first, we verify that temperature at each level does not increase monotonically in the calculation by using modified programs. Fig.2 shows time evolution of horizontal mean temperature from 0 sec to  $8.64 \times 10^5 \text{ sec}$  at altitudes of 5 km (red), 10 km (green), 15 km (blue), and 20 km (black), respectively. Fig.2 indicates that the horizontal mean temperature at each level does not increase monotonically. This characteristic means that the program bug in the radiation scheme is fixed.

Next, we verify conservation of total mass of gas and cloud. In general, the total mass is not conserved in the quasi-compressible system. The equation of mass balance is given by

$$\frac{\partial}{\partial t} \iint_V (\rho + \rho_s) dV \simeq \iint_V \frac{\bar{\rho}}{\bar{\theta}} \left( u' \frac{\partial \theta'}{\partial x} + w' \frac{\partial \theta'}{\partial z} \right) dV, \quad (16)$$

where the integral in (16) is performed over all area. The value of the term of the right hand in (16) is estimated to be about 0.44 kg/sec. Fig.3 shows time evolution of total mass. The total mass increases at the rate of about 0.23 kg/sec on the average. The rate of increase of the total mass is of the same order of the value estimated theoretically, therefore in our calculation, mass conservation is not violated. The characteristic means that the program bug in the condensation scheme is fixed.

In order to confirm whether a quasi-equilibrium state is obtained or not, time evolutions of total kinetic energy and total cloud mass are examined. Fig.4 shows time evolution of total kinetic energy. Total kinetic energy increases monotonically until about  $3.0 \times 10^5$  sec, and it is nearly constant after the time. Fig.5 shows time evolution of total cloud mass. Total cloud mass increases monotonically until about  $2.8 \times 10^5$  sec, and thereafter it is nearly constant. Thus, it seems that a quasi-equilibrium state is obtained at about  $3.0 \times 10^5$  sec.

We describe here time evolution of cloud density and vertical velocity. Fig.6a, 6b and 6c show distributions of cloud density at  $2.16 \times 10^4$ ,  $8.64 \times 10^4$ , and  $3.03 \times 10^5$  sec, respectively. Fig.7a, 7b and 7c show distributions of vertical velocity at  $2.16 \times 10^4$ ,  $8.64 \times 10^4$ , and  $3.03 \times 10^5$  sec, respectively. In the early stage, isolated clouds are formed in ascent regions near 6 km height (Fig.6a, 7a). Thereafter, vertical velocity and cloud density increase, and clouds grow up in the vertical direction (Fig.6b, 7b). Vertical velocity continues to increase until cloud distribution becomes horizontally uniform (Fig.6c, 7c), and thereafter becomes nearly constant temporally. After about  $3.03 \times 10^5$  sec, the region above 7 km level is covered with clouds. One-cell circulation in which maximum vertical velocity is about 15 m/sec develops in the cloud layer. Around 7 km height, the cloud layer is sustained by the balance of negative contribution of evaporation and positive contribution of advection. At altitudes above 7 km, the cloud layer is sustained by the balance of negative contribution of advection and

positive contribution of condensation.

## 5 Concluding Remarks

We perform the recalculation of Yamashita *et al.* (2009) by using the modified programs so as to maintain heat budget and mass conservation. Our calculation shows that moist convection does develop in the case of  $S_{cr} = 1.0$  (Fig.6b). This result is different from the discussion by Colaprete *et al.* (2003) that moist convection does not develop for  $S_{cr} = 1.0$ . In order to investigate the mechanism for development of the moist convection, detailed analysis will be required. For further works, we are going to perform parameter sweep experiments for critical saturation ratio, and calculations with considering the falling of cloud particles. Since numerical experiments of cloud convection such as Nakajima *et al.* (1998) showed that the falling of cloud particles affects the convective structure, calculations with considering these effects are essential to investigate the structure of the convection which is established through a large number of life cycles of convective cloud elements.

## Acknowledgement

Figures are plotted by using the softwares developed by Dennou Ruby Project (<http://ruby.gfd-dennou.org/>). Numerical calculations are performed by the NEC SX9 of the ISAS/PLAIN Center, JAXA.

## References

- Asselin, R., 1972: "Frequency filter for time integrations", *Mon. Wea. Rev.*, **100**, 487 – 490.
- Colaprete, A., Toon, O. B., 2002: "Carbon dioxide snow storms during the polar night on Mars", *J. Geophys. Res.*, **107**, 5051, doi:10.1029/2001JE001758.
- Colaprete, A., Haberle, R. M., Toon, O. B., 2003: "Formation of convective carbon dioxide clouds near the south pole of Mars." *J. Geophys. Res.*, **108**(E7), 5081, doi:10.1029/2003JE002053
- Forget, F., Pierrehumbert, R. T., 1997: "Warming early Mars with carbon dioxide clouds that scatter infrared radiation", *Science*, **278**, 1273 – 1276.

- Glandorf, D. L., Colaprete, A., Tolbert, M. A., Toon, O. B., 2002: "CO<sub>2</sub> snow on Mars and early Earth: experimental constraints", *Icarus*, **160**, 66 – 72.
- Kasting, J. F., "CO<sub>2</sub> condensation and the climate of early Mars", *Icarus*, **94** (1991), pp. 1 – 13.
- Klemp, J. B., Wilhelmson, R. B., 1978: "The simulation of three-dimensional convective storm dynamics", *J. Atmos. Sci.*, **35**, 1070 – 1096.
- Mitsuda, C., 2007: "The greenhouse effect of radiatively adjusted CO<sub>2</sub> 'ice cloud in a Martian paleoatmosphere"(in Japanese), Doctoral thesis of Division of Earth and Planetary Sciences, Graduate School of Science, 115 pp.
- Nakajima, K., Takehiro, S., Ishiwatari, M., Hayashi, Y.-Y., 1998: "Cloud convections in geophysical and planetary fluids"(in Japanese), *Nagare Multimedia*, <http://www2.nagare.or.jp/mm/98/nakajima/index.htm>
- Nakajima, K., Takehiro, S., Ishiwatari, M., Hayashi, Y.-Y., 2000: "Numerical modeling of Jupiter's moist convection layer", *Geophys. Res. Lett.*, **27**, 3129–3132.
- National Astronomical Observatory of Japan, 2004: "Chronological scientific tables " (in Japanese), *Maruzen*, 1015 pp.
- Odaka, M., Kitamori, T., Sugiyama, K., Nakajima, K., Takahashi, Y. O., Ishiwatari, M., Hayashi, Y.-Y., 2005: "A formulation of non-hydrostatic model for moist convection in the Martian atmosphere", Proceeding of the 38 th ISAS Lunar and Planetary Symposium, 173 – 175.
- Odaka, M., Kitamori, T., Sugiyama, K., Nakajima, K., Hayashi, Y.-Y., 2006: "A numerical simulation of Martian atmospheric moist convection"(in Japanese), Proceeding of the 20 th ISAS Atmospheric Science Symposium, 103 – 106.
- Pollack, J. B, Kasting, J. F., Richardson, S. M. and Poliakov, K., 1987: "The case for a wet, warm climate on early Mars", *Icarus*, **71**, 203 – 224.
- Sugiyama, K., Odaka, M., Nakajima, K., Hayashi, Y.-Y., 2009: "Development of a cloud convection model to investigate the Jupiter's atmosphere", *Nagare Multimedia*, <http://www2.nagare.or.jp/mm/2009/sugiyama/index.htm>
- The society of chemical engineers of Japan, 1999: "The handbook of chemistry and engineering"(in Japanese), *Maruzen*, 1339 pp.
- Tobie, G., Forget, F., Lott, F., 2003: "Numerical simulation of winter polar wave clouds observed by Mars Global Surveyor Mars Orbiter Laser Altimeter", *Icarus*, **35**, 33 – 49.
- Yamashita, T., Odaka, M., Sugiyama, K., Nakajima, K., Ishiwatari, M., Hayashi, Y.-Y., 2009: "A numerical simulation of Martian atmospheric moist convection", Proceeding of the 42 th ISAS Lunar and Planetary Symposium, 12 – 16.

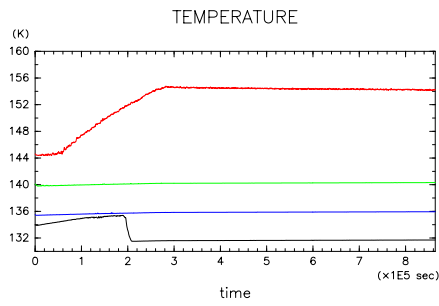


Figure 2: Time evolution of horizontal mean temperature from 0 sec to 864000 sec. Red, green, blue and black lines correspond to the temperature at altitudes of 5 km, 10 km, 15 km, and 20 km, respectively.

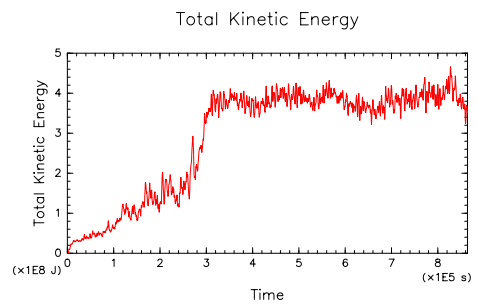


Figure 4: Time evolution of total kinetic energy from 0 sec to  $8.64 \times 10^5$  sec.

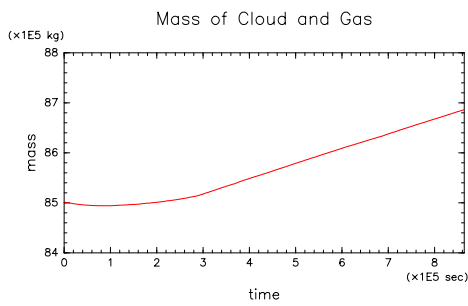


Figure 3: Time evolution of the sum of the total gas mass and cloud mass from 0 sec to  $8.64 \times 10^5$  sec.

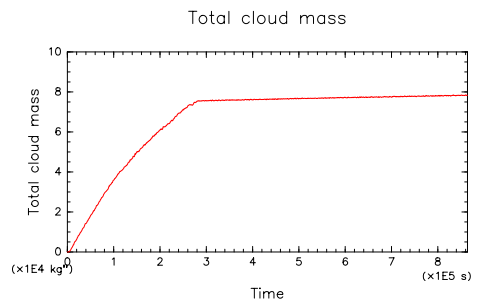


Figure 5: Time evolution of total cloud mass from 0 sec to  $8.64 \times 10^5$  sec.

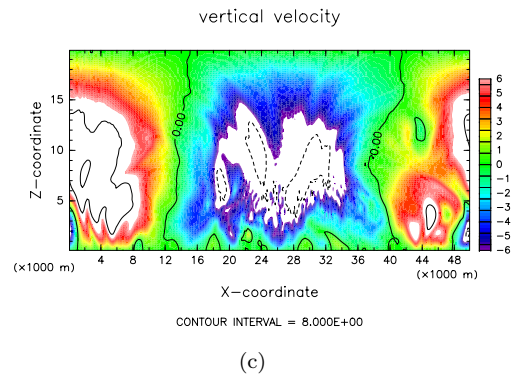
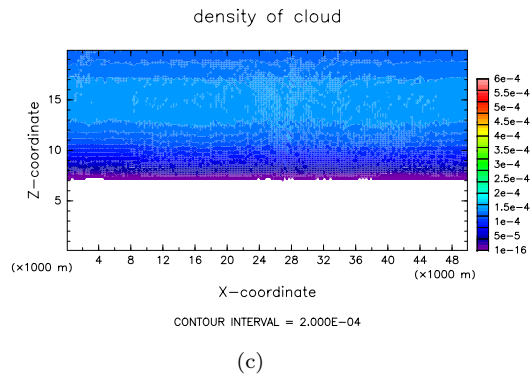
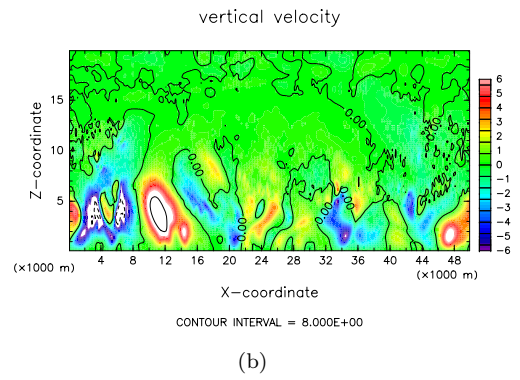
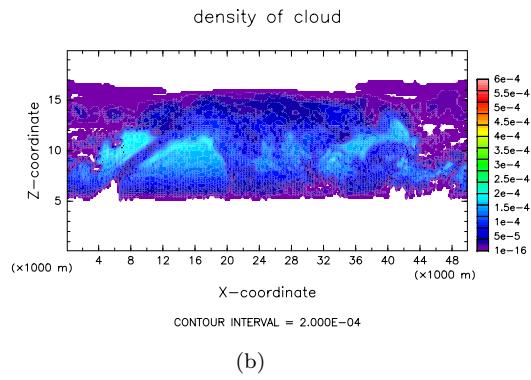
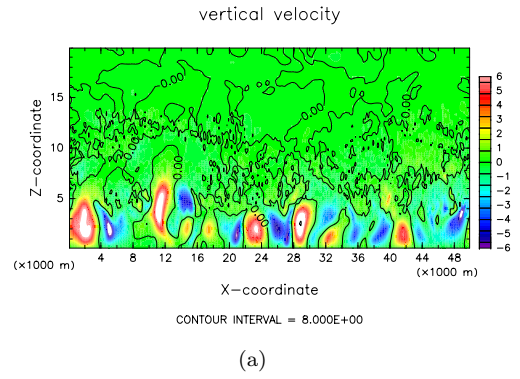
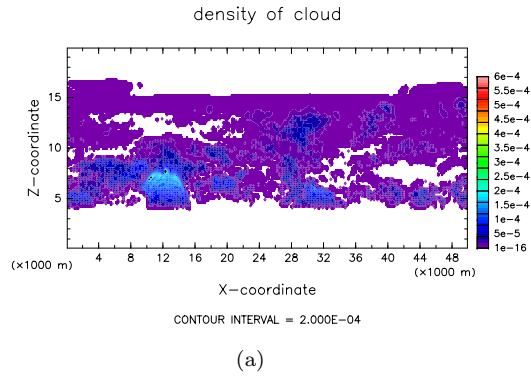


Figure 6: Snapshots for distribution of density of cloud [kg / m<sup>3</sup>] at : (a)  $2.16 \times 10^4$  sec, (b)  $8.64 \times 10^4$  sec, (c)  $3.03 \times 10^5$  sec.

Figure 7: Snapshots for distribution of vertical velocity [m/sec] at : (a)  $2.16 \times 10^4$  sec, (b)  $8.64 \times 10^4$  sec, (c)  $3.03 \times 10^5$  sec.